Marine Pollution Bulletin 183 (2022) 114061

Contents lists available at ScienceDirect

Marine Pollution Bulletin

journal homepage: www.elsevier.com/locate/marpolbul

Development of an analytical procedure to analyze microplastics in edible macroalgae using an enzymatic-oxidative digestion

Adrián López-Rosales, Jose M. Andrade *, Purificación López-Mahía, Soledad Muniategui-Lorenzo

Grupo Química Analítica Aplicada (QANAP), Instituto Universitario de Medio Ambiente (IUMA), Universidade da Coruña, Campus da Zapateira, E-15071 A Coruña, Spain

ARTICLE INFO

Keywords:
Microplastics
Macroalgae
Seaweeds
Enzymatic digestion
IR microspectroscopy

ABSTRACT

Besides being food and a refuge to marine species, macroalgae are a powerful and renewable economic resource. However, they may introduce microplastics (MPs) in the trophic chain. We developed a reliable analytical method to characterize and quantify MPs in common and edible macroalgae. Several digestion methods and filters, along with various measurement options, were studied. A new enzymatic-oxidative protocol with a unique final filtration was selected and validated with a mixture of 5 commercial macroalgae (*Undaria pinnatifida spp, Porphyra spp, Ulva spp, Laminaria ochroleuca and Himanthalia elongate*). Further, it was shown that washing the macroalgae to release MPs is suboptimal and the potential adhesion of MPs to macroalgae was evaluated. A filter subsampling strategy that scans 33.64 % of its surface reduced the time required to characterize <70 μm particles and fibres directly on the 47 mm diameter filter using an IR microscope (1 sample/day).

1. Introduction

Microplastics (MPs) already constitute a true concern to all ecosystems (Picó and Barceló, 2019; Weis, 2019), and their presence was reported in all types of marine animals, not only due to direct ingestion but because of trophic transfer (Walkinshaw et al., 2020); e.g., from molluscs to various types of fish (Yu et al., 2020). However, studies dealing with the presence of MPs at the very basis of the trophic chain are not too abundant. Some reports focused on plankton (López-Rosales et al., 2021; Rodrigues et al., 2021) but research on macroalgae is still developing (Gao et al., 2020, 2021b). This contrasts with the ecological and economic importance of (macro)algae (Gao et al., 2021a) and the fact that they can retain MPs (Feng et al., 2020b; Gutow et al., 2016; Peller et al., 2021; Seng et al., 2020; Sundbæk et al., 2018).

In effect, some species of macroalgae form marine forests of major ecological importance (Bertelli and Unsworth, 2014; Huang et al., 2020; Jones et al., 2020). As a matter of example, *Posidonia oceanica* (in the Mediterranean Sea) and *Laminaria* sp. (oriental Atlantic Marine forests) in the Iberian Peninsula (Blanco Murillo, 2018) can serve as the basement for the entire food chain. They offer also a refuge for animals (Peteiro and García Tasende, 2015). But algae are not only important at the ecosystem level, they also reach high economic importance (Feng et al., 2020b) as raw materials for the cosmetics and food industries. Various macroalgae or seaweed species (please, note that both terms are used indistinctly throughout this work to avoid strong repetition) are of high culinary interest due to their flavour and nutritional profile (Peñalver et al., 2020; Gao et al., 2019). MPs have been found attached to algae living in natural conditions. Goss et al. (2018) reported that 75 % of the specimens of *Thalassia testudinum* collected in Belize contained up to 3.69 ± 0.99 plastic fibres and 0.75 ± 0.25 plastic particles per leaf. Jones et al. (2020) detected 4.25 ± 0.59 MPs per leaf in *Zostera marina* seaweeds where the main polymer was PET, with higher MPs loads than corresponding sandy sediments. Peller et al. (2021) found 34 microfibres/g in lakes Erie and Michigan, two- to four-fold higher than in water and sediments (Peller et al., 2019).

Seng et al. (2020) detected MPs in three seagrass species (*Cymodocea rotundata, Cymodocea serrulata and Thalassia hemprichii*) and two macroalgae species (*Padina* sp. *and Sargassum ilicifolium*) from an urbanised intertidal zone. Remarkably, in the former 38.7 % of the leaves were contaminated by at least one MP, mostly microfibres (97.3 %).

Li et al. (2020) found 1.8 ± 0.6 MPs/g (dry weight) in *Pyropia yezoensis* (for human consumption) upon arrival at the factory, mainly PP fibres. After processing (commercial form) PET fibres predominated. In another research they considered 5 types of macroalgae (*Gracilaria*

* Corresponding author.
E-mail address: andrade@udc.es (J.M. Andrade).

https://doi.org/10.1016/j.marpolbul.2022.114061
Received 30 May 2022; Received in revised form 20 July 2022; Accepted 17 August 2022
Available online 30 August 2022

lemaneiformis, Chondrus ocellatus, Ulva lactuca, Ulva prolifera, Saccharina japonica) and found as high averages as 1243 ± 1394 MPs/Kg·dw (using a digestion method procedure), and 58.8 MPs/Kg·dw picking up directly MPs from the algal surface (Li et al., 2022).

Feng et al. (2020a) reported 0.12–0.17 MPs/g (wet weight) on seaweed samples; in particular, for *U. prolifera* they found 0.83 ± 0.95 MPs/g (wet weight), mostly microfibres, 595–3917 times higher than those found in the sea. Gao et al. (2020) reported the ability of this seaweed to retain MPs so that Li et al. (2022), suggested that it could be used for bioremediation.

The capability of seaweed beds to accelerate/facilitate particle sedimentation and to adsorb particles floating on waves make them a hotspot for monitoring studies (Huang et al., 2020; Gao et al., 2020; Li et al., 2022). Thus, Huang et al. (2020) reported more MPs in sediments populated by *Enhalus acoroides* than in unpopulated ones. In addition, typical algal strandings at the coastline can be a strong indicator of MPs at seawater (Cozzolino et al., 2020).

A brief review on the reasons why (macro)algae adsorb MPs is in order. However, this is not the focus of the paper and interested readers are kindly forwarded to references cited hereinafter. Several hypotheses are based on the gel-like properties provided by the alginates, in the form of a mucus layer of polysaccharides in the cell wall (Feng et al., 2020b; Feng et al., 2020a; Gutow et al., 2016a; Peller et al., 2021; Seng et al., 2020). The presence of cellulose, pectin, xylose or glucose can also contribute (Peller et al., 2021). Additional mechanisms involve physical entanglement between branches (as observed in *Cladophora* (Peller et al., 2021) or *U. prolifera* (Feng et al., 2020a)), or trapping in air sacs (such as *Sargassum horneri*; Feng et al., 2020a). It has also been proposed that the phaeophycean microvilli of *Fucus* sp. may trap MPs (Gutow et al., 2016; Sundbæk et al., 2018).

Several authors suggested that the electrostatic properties of MPs and cellulose also play an important role in adsorption (Sundbæk et al., 2018; Gutow et al., 2016; Peller et al., 2021; Bhattacharya et al., 2010; Nolte et al., 2017). Other authors (Jones et al., 2020; Gutow et al., 2016; Peller et al., 2021) suggested that the epiphytes present in the seagrass may easily adhere to the sticky biofilms present on MPs. It seems that structurally complex stems of macroalgae increase the capacity to adsorb particulate matter (Boney, 1978; Gutow et al., 2016; Li et al., 2022). Li et al. (2022) proposed 5 types of adsorption pathways: wrapping, embedment, attachment, entanglement an entrapment by epibionts and, likely, all of them contribute (Peller et al., 2021).

In laboratory conditions a correlation was found between the retained MPs and the number of suspended MPs (Gutow et al., 2016). For example, the percentage of adhesion of plastic particles ranged from 16 to 112 % (Sundbæk et al., 2018). Li et al. (2020) demonstrated adhesion of up to 10 items/cm^2 on *P. yezoensis* (used to make Nori). Peller et al. (2021) showed that *Cladophora* accumulates twice as many MPs in the algae as in the water after 15 h. As all these experiments worked with very high concentrations of MPs in water their representativeness with respect to natural situations is still unclear. However, the resistance of MPs to leave algae was demonstrated by Peller et al. (2021) as the fibres contained in the algae were not detached after washing with water.

The ability of algae to retain MPs may have obvious implications for the food chain (Seng et al., 2020), but studies are still lacking. Trophic transfers were reported from *Fucus vesiculosus* to marine gastropods (periwinkle) *Littorina littorea* (Gutow et al., 2016); macroalgae coprophagous isopods (Hämer et al., 2014); and cellulose fibres from *P. oceanica* seagrass to amphipods (Remy et al. (2015). Goss et al. (2018) and Jones et al. (2020) argued that epibionts could ingest MPs and, then, transfer them to higher trophic levels. Furthermore, the adherence of MPs to algae may lead to the transference of other pollutants, such as additives (phthalates, BPA, etc.) (Gutow et al., 2016; Roberts et al., 2006). In addition, there are several species of algae that are consumed by fish (Feng et al., 2020b). Whether this problem can reach humans needs to be studied deeper (Sana et al., 2020). Most studies cited above considered ad-hoc methodologies to isolate, first, and characterize, then, the MPs. Nevertheless, the common washing approaches are far from being accepted and most people digest the organic matter of the algae. The lack of a harmonized protocol makes comparability of the results cumbersome and, so, the present paper focuses on developing a validated and reliable analytical procedure to address sample treatment and subsequently characterize MPs.

Therefore, the major objectives of the present study are to develop a digestion method suitable for a variety of edible seaweeds, and to optimise the measurement time in a sequential IR microscope by proposing a subsampling strategy for smallest MPs.

The paper is organized so that general, common methodological issues are addressed first. This includes selection of the filter and how to measure the particles retained on it, Section 3.2, where from a novel approach is presented to speed the measurement process when a single-point IR microscope is used. Then, sample pretreatment is studied (including traditional algae washing) and three digestion methods for the algae are considered (Section 3.3). Finally, some conclusions are presented.

2. Experimental part

2.1. Materials and reagents

The reagents used for the alkaline treatment were KOH (Panreac), and Triton X-100 (Sigma-Aldrich). The enzymatic treatment required sodium dodecyl sulfate (SDS ≥ 98.5 % purity), Tris (tris(hydroxymethyl) aminomethane), *Streptomyces griseus* protease (Type XIV activity ≥ 3.5 units/mg), and aspergillus niger cellulase (0.8 U/mg), all them were from Sigma-Aldrich. SDS (2 % w/w) and Tris (1 M) working solutions were employed. The pH = 5 buffer solution was prepared using acetic acid (Panreac) and sodium acetate trihydrate (Sigma-Aldrich). H_2O_2 (≥30 %) was from Sigma-Aldrich.

AE100 Whatman cellulose nitrate filters (12 μm pore diameter, 47 mm filter diameter) and Bopp stainless steel filters (20 μm mesh, 47 mm filter diameter, Bopp&Co. AG, Switzerland) were used and stored in 60/15 mm glass Petri dishes from Pobel. The seaweed samples were prepared in 1 L Pobel bottles and 1 L Pobel Erlenmeyers were used for sample digestion and incubation.

2.2. Apparatus

The incubation system was a Rotabit P (Selecta, Spain), with temperature and agitation controls. A Pobel vacuum filtration system was used in combination with a Millipore vacuum pump. A 2001 micropH-meter from Crison (Barcelona, Spain) calibrated in each working session was employed throughout. The lyophilization system was a LYPH-LOCK 6 L freeze-dry system, model 77,530, from Labconco Corp. (Kansas City, MO). The optical analysis used a Leitz Wetzlar stereomicroscope (10× ocular and manual adjustment of the objective zoom up to 5×, total magnification 50×). The IR analysis was performed with a Spotlight 200i Perkin Elmer microscope coupled to a Spectrum 400FTIR Perkin Elmer spectrometer equipped with an MCT detector. The images obtained with the micro-FTIR were treated with the Perkin Elmer Spectrum software.

The FTIR experimental set up was (following the proposed minimum information for publication of IR-related data on MPs characterization, MIPIR-MP (Andrade et al., 2020)): 4000–600 cm^{-1} working range; nominal resolution: 4 cm^{-1}; number of scans: 100; strong Beer-Norton apodization; reflectance mode; apertures: 70 × 70 for particles and 10 × 100 for fibres; spectral processing: background correction normalization 10 % and Kubelka-Munk transformation.

2.3. Samples

Five common and edible macroalgae in Galician ecosystems -*Undaria*

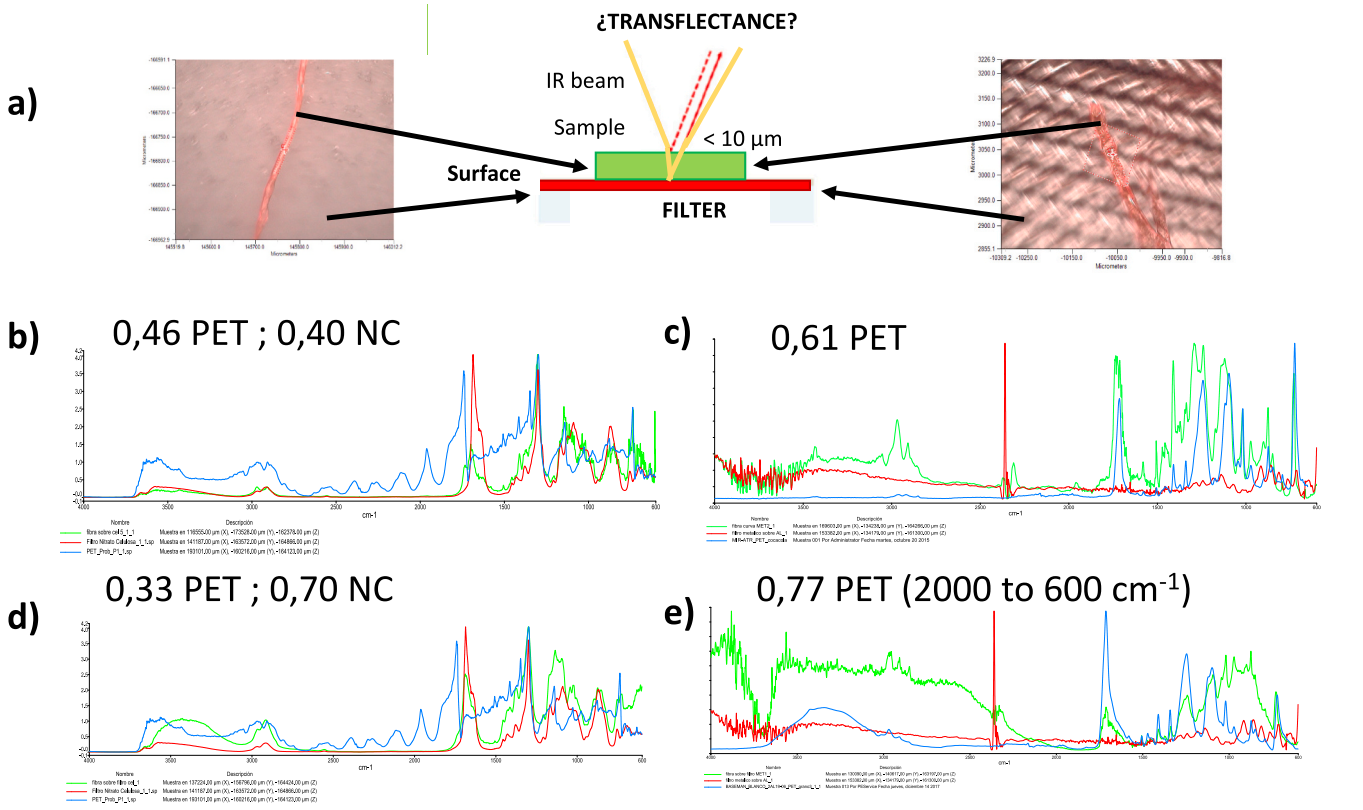

Fig. 1. Concept of transflectance vs. reflectance (a). Match index of the spectrum of a PET fibre measured over a nitrocellulose filter –NC- (b and d) and over a metallic one (c and e). For the former the correlation against the spectrum of the filter matrix is also given (NC). Spectral codes: Red = filters, blue = reference PET, green = samples. (For interpretation of the references to color in this figure legend, the reader is referred to the web version of this article.)

pinnatifida spp (Wakame), *Porphyra spp* (Nori), *Ulva spp* (Sea Lettuce), *L. ochroleuca* (Kombu) and *Himanthalia elongata* (Sea Spaghetti)- were collected from commercialized products (Porto Muiños, ecological seaweeds from the Galician coast). They were mixed in the laboratory so as to obtain a composite sample with a variety of typical seaweeds that will be treated with a unique protocol. These were prepared weighing 1 g of each type of dried algae and hydrated in 500 mL of filtered seawater (through 1 µm filters), this yielded 27 g of algae, wet weight.

Five replicates were prepared and spiked with 20 particles of 250–350 µm of PP, PS, PA, PET and PE; in addition, 20 particles of 70–80 µm of PVC and 20 PET fibres (8–10 µm thick and about 2.5 mm long) were added. Note that the fibres are a bit long but this allowed for their straightforward and highly reproducible manual preparation in the laboratory, without major visual differences among them. Those values correspond to 0.28 MPs/mL (4.4 MPs/g wet algae) and 0.04 fibres/mL (0.75 fibres/g wet algae), which are higher than those expected for samples at the Spanish Atlantic coastal waters (Mendoza et al., 2020), but similar to the effluents from wastewater discharges (Franco et al., 2020).

All those mixtures were agitated for 24 h at 120 oscillations/min under a rotative movement, subsequent resting for 24 h and agitated again for 24 h under a sway movement. The objective was to promote a continuous contact between the MPs and the algal surface although considering longer contact time between the MPs and the algae than previous studies (Gutow et al., 2016; Li et al., 2020; Peller et al., 2021; Sundbæk et al., 2018).

2.4. Quality control

Extran MA01 alkaline soap was used to clean all material (48 h, rinsed with tap and Milli-Q water before and during all working steps). Aluminium foil was used to protect all materials. All solutions were made with fresh ultrapure Milli-Q water and manipulations were carried out inside dedicated fume hoods. Cotton cloths were employed as far as possible to avoid contamination with synthetic fibres. Stainless steel filters were washed following the protocol described by Enders et al. (2020), although with Triton-X100; in addition, they were subjected to 450 °C for 4 h (Liu et al., 2019). Procedural blanks were made on each working season considering all reagents and filtration instruments (Hermsen et al., 2018). Cellulose and co-polymer fibres from the laboratory environment were detected, although particles were absent from all blank filters. 3 L of mili Q water were employed in the filtration processes.

2.5. Statistical analysis

The statistical studies were done using SPSS, v27, from IBM. All the tests were performed at a 95 % confidence level.

3. Results and discussions

In the next paragraphs, the common methodological issues, related in essence to the measurement stage, are addressed first (Sections 3.1 and 3.2) whereas those aspects related to algae treatment and digestion are considered next (Section 3.3).

3.1. Selection of the filters

In this paper infrared reflectance measurements were selected because of their operational simplicity. However, this reduced the types of filters that can be used since, for example, cotton or glass fibre should be discarded because they trap particles in their 3D structures. But even those that retain the particles over their surface (e.g., cellulose nitrate or nylon) yielded problems in the reflectance spectra of the smallest

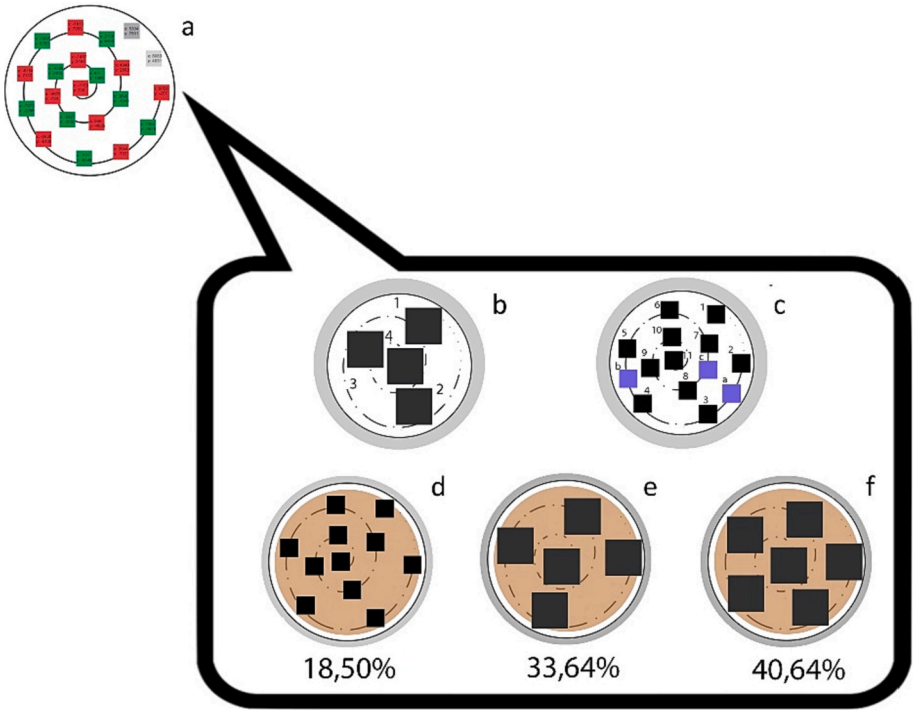

Fig. 2. Filter subsampling patterns studied in this paper. The pattern covering 33.64 % of filter was selected here and it considers five 1 cm^2 squares in an helical pattern. a) original pattern proposed by Huppertsberg and Knepper; b–f) scanning patterns studied here using 25 mm^2 (c and d) and 1 cm^2 (b, e and f) areas.

particles whenever they are measured directly at the filter (even when the filter itself was included in the background). This was attributed to the fact that the fibres under study had a very small diameter (ca. 10 μm) which is very close to, or equals, the practical mid-IR light focusing capabilities of the micro-IR instrument (and, so, the IR beam impacts not only at the particle but at its surroundings). Further, for small particles it is highly possible that the "reflectance" spectrum contains transflectance characteristics (see Fig. 1 for a conceptual scheme of this idea). This means that the signal of the filter contributes to the overall spectrum; mainly at the fingerprint region where, for instance, nitrate cellulose peaks overlap with those of some polymers. This caused poor correlations when those spectra were matched to the database (detailed results not reported here). Even, some PET fibres showed better correlations with nitrocellulose than with the polymer itself. In addition, recall that small instrumental apertures to measure fibres render noisy spectra, as they imply very low energy outputs. For big particles (ca >50 μm) the influence of the filter background was not observed, likely because "true" reflectance spectra were obtained.

To avoid those problems, studies were done using stainless steel filters and it was seen that they did not affect the spectra of the particles, noise got reduced and good spectral correlations were obtained (these can be improved further by restricting the working range to the 2000–600 cm^{-1} spectral region, Fig. 1). As a result, the recorded spectra of the fibres correlated acceptably well with the PET in the database (0.60 ± 0.11, n = 18, the ± refers to 1SD). On the contrary, the correlations when using nitrate cellulose filters were poor (0.33 ± 0.07).

3.2. Measurement of the filter

Commercial IR microscopes can only map filter areas of around 400 × 500 μm. Registering successive adjacent areas allow for images as large as 1 cm^2. In our case this took about 20 min. However mapping the overall typical filter (47 mm diameter) would imply such a long time that it is not feasible for routine purposes; not to mention the software limitations in terms of required memory and computer time, and the technical difficulties for measurement (e.g., liquid nitrogen supply to the detector). As a matter of example, to benchmark the filter subsampling strategy depicted below, the IR microscope required –at least- a week per each 47 mm filter, that is not feasible for monitoring measurements. Consequently, two filter measurement strategies were devised to characterize and count the number of MPs over them: manual particle location and filter subsampling. Both were assessed spiking Mili-Q water (500 mL) with 20 MPs of PVC and 20 PET microfibres per sample.

3.2.1. Manual particle location

In this approach, the entire filter is visualized through a stereomicroscope and suspicious particles are picked up with microtweezers and placed in individual cavities of dedicated multiwell aluminium plates developed in our laboratory (they had already been presented at López-Rosales et al., 2021). Next, the controlling software of the IR system is used to locate each particle in the plate and subsequently measure them automatically. This saves a lot of time when working with the IR microscope. This methodology was validated satisfactorily for particles >70 μm (López-Rosales et al., 2021) and it is a very appealing and straightforward solution whenever marine monitoring campaigns are undertaken because, usually, they employ manta trawls and Newston nets whose collecting mesh sizes are ca. 330 μm (Carretero et al., 2022).

3.2.2. Filter subsampling

To take account of small (<70 μm) particles and fibres in a reasonable time, not easily handled manually, it is necessary to sample a fraction of the filter and then extrapolate the results. This obviously rises concerns on the representativity issue (Brandt et al., 2020). Selecting a 1 cm^2 region for mapping is not enough regardless of its position. Thus, Huppertsberg and Knepper (2020) proposed a helical pattern that scans between 8 % and 20 % of the filter (Fig. 2a), although Brandt et al. (2021) advised to measure at least 50 % of the filter to keep the error < 20 %.

The former pattern was redesigned to adapt it to the working characteristics of the Spotlight 200i, for a 47 mm diameter filter. The percentage of filter sampled was increased and different designs were tested, taking into account the two maximum individual image sizes that

Table 1
Statistical results associated to the validation of the selected filter subsampling strategy (n = 15). The averages and standard deviations (SD) are in %.

	Fibres ± SD	Particles ± SD
Average recovery (the number of particles at the entire filter are counted)	89 ± 4	97 ± 3
Average recovery (number of particles counted using the filter subsampling strategy)	86 ± 26	94 ± 26
Average of relative error of the filter subsampling strategy (n = 15)	3 ± 32	−3 ± 27
Average of absolute error of the filter subsampling strategy (n = 15)	−3 ± 28	−3 ± 26
Shapiro-Wilk's normality test for the 15 recoveries calculated for the selected subsampling strategy (p-value)	0.509	0.110
Levene's test (variance of the filter subsampling vs variance of the entire filter, p-value)	0.0004	2×10^{-7}
Student's *t*-test (number of particles for the filter subsampling vs number of particles for the entire filter, p-value)	0.669	0.659

Table 2
Recoveries (%) (± standard deviation, n = 5) obtained using the 'filter subsampling' and the 'entire filter' quantification strategies after an enzymatic-oxidative matrix digestion of a true sample (see Section 3.3.2 for details).

		Filter subsampling (n = 5)			Entire filter (n = 5)		
		PVC (20)	Fibres (20)	All MP (40)	PVC (20)	Fibres (20)	All MP (40)
Washing	Algae	12 ± 13	10 ± 7	11 ± 4	9 ± 10	9 ± 5	9 ± 7
	Water	51 ± 13	45 ± 18	48 ± 16	59 ± 5	53 ± 10	56 ± 8
	Total matrix	60 ± 18	55 ± 14	57 ± 16	69 ± 11	64 ± 7	66 ± 10
Digestion	Algae	27 ± 12	32 ± 17	30 ± 12	33 ± 6	27 ± 8	30 ± 6
	Water	60 ± 15	51 ± 13	55 ± 7	56 ± 7	58 ± 16	55 ± 8
	Total matrix	87 ± 22	83 ± 24	85 ± 16	89 ± 4	85 ± 8	87 ± 5
Student's *t*-test (filter subsampling vs entire filter, p-value)	Washing	PVC	0.384				
		Fibres	0.247				
		All MP	0.345				
	Digestion	PVC	0.852				
		Fibres	0.867				
		All MP	0.800				

the Spotlight-200i can compose automatically (100 mm^2 and 25 mm^2), see Fig. 2.

To decide which pattern yielded best predictions fifteen essays were performed per configuration. The first two subsampling patterns (Fig. 2b and c) gave representativity problems due to the tendency of the fibres to stay at the edge of the filter, and that region was not sampled properly. Pattern d in Fig. 2 uses 18.50 % of the filter and it was rejected because its errors and standard deviations were > 30 %. In addition, performing eleven image compositions of 25 mm^2 demands high dedication time for the operator. The pattern covering 40.64 % of the filter (Fig. 2f) was discarded because it exceeded the time of a regular working day (7 h) so it is not feasible currently.

Hence, the option of sweeping 33.64 % of the filter was chosen (Fig. 2e). It involves 5 automatic mappings of 100 mm^2 but the final procedure is quite fast since each image takes about 20 min to be composed. Then, at each squared mapping area the user selects the particles to be measured and they are scanned automatically (around 1 h per square in our study). The final number of particles is extrapolated by multiplying times 2.97. Table 1 presents the results associated to the selected filter subsampling pattern. The overall errors were calculated as averages of 15 replicates (from scratch), considering the equations below (note that the absolute error of the measurement is not the absolute value of error and, so, it has algebraic sign and its average represents the average bias).

$$\textit{Relative error of filter subsampling} = \frac{\textit{subsampling } MPs_i - \textit{entire filter } MPs_i}{\textit{entire filter } MPs_i} \times 100$$

$$\text{Absolute error of filter subsampling} = \text{subsampling } MPs_i - \text{entire filter } MPs_i$$

In these equations 'subsampling MPs_i' refers to the number of MPs counted in the subsampling pattern under study 'i', while 'entire filter MPs_i' is the number of MPs counted on the overall filter in assay 'i' (here, i is the number of replicates, 1 … 15).

As a general conclusion it can be seen that the filter subsampling strategy leads to equivalent recoveries (Student's *t*-test 95 % confidence) than the overall filter measurement (>85 % and >90 % for fibres and particles, respectively). However, it is also worth noting that the standard deviations associated to filter subsampling increase as well, and they are significantly different (Levene's test <0,05). Thus, although the average absolute relative errors are really very low (<5 %), the dispersion of the results is around 25 %.

In addition, Table 2 presents another study that confirms the good results of the selected filter subsampling strategy. Please, note that the particular details of this case study will be detailed in next section; for now, just consider the last raw of the digestion data, labelled as 'Total matrix'. The average recoveries for this spiked sample were slightly lower than those at Table 1 but, nevertheless, their confidence intervals overlap even at the stringent 68 % confidence level (i.e., ±1SD). Hence, there were no significant differences in the average of recoveries of 5 replicates (Student's *t*-test, 95 % confidence) between the two filter measurement strategies. The term 'Entire filter' involves a full and time-consuming overall filter measurement, as mentioned at the onset of this section.

Finally, as a pragmatic working rule, in our view the number of MPs in a filter can be estimated reliably and quite straightforwardly using a two steps procedure: 1st: search the entire filter for >70 μm particles using a stereomicroscope and pick-up them to multiwell aluminium plates; characterize them using IR microspectroscopy; 2nd: take account of smallest particles and fibres by subsampling them directly on the metallic filter, covering 33.64 % of its surface.

In this way it is possible to characterize a filter (ideally, a sample) per working day, as long as the subset of particles to be characterized does not exceed too much from 140 particles. The time can be reduced significantly if the number of scans per particle is reduced (in this work, we used 100 scans/spectrum), but that might yield poorer spectral quality –more doubtful assignations/matches- and has to be checked on an ad-hoc basis.

3.3. Sample treatment procedures

To emulate current working procedures during field sampling the seaweed suspensions were freezed. Then, freeze-drying was tested as a way to remove water (Enders et al., 2020) but that took ca. 5 days. Therefore, it was decided not to proceed in that way but to separate the solid and liquid phases by sieving (1 mm metallic mesh, Fig. 3a), the flask with the water phase was filtered again through a stainless steel

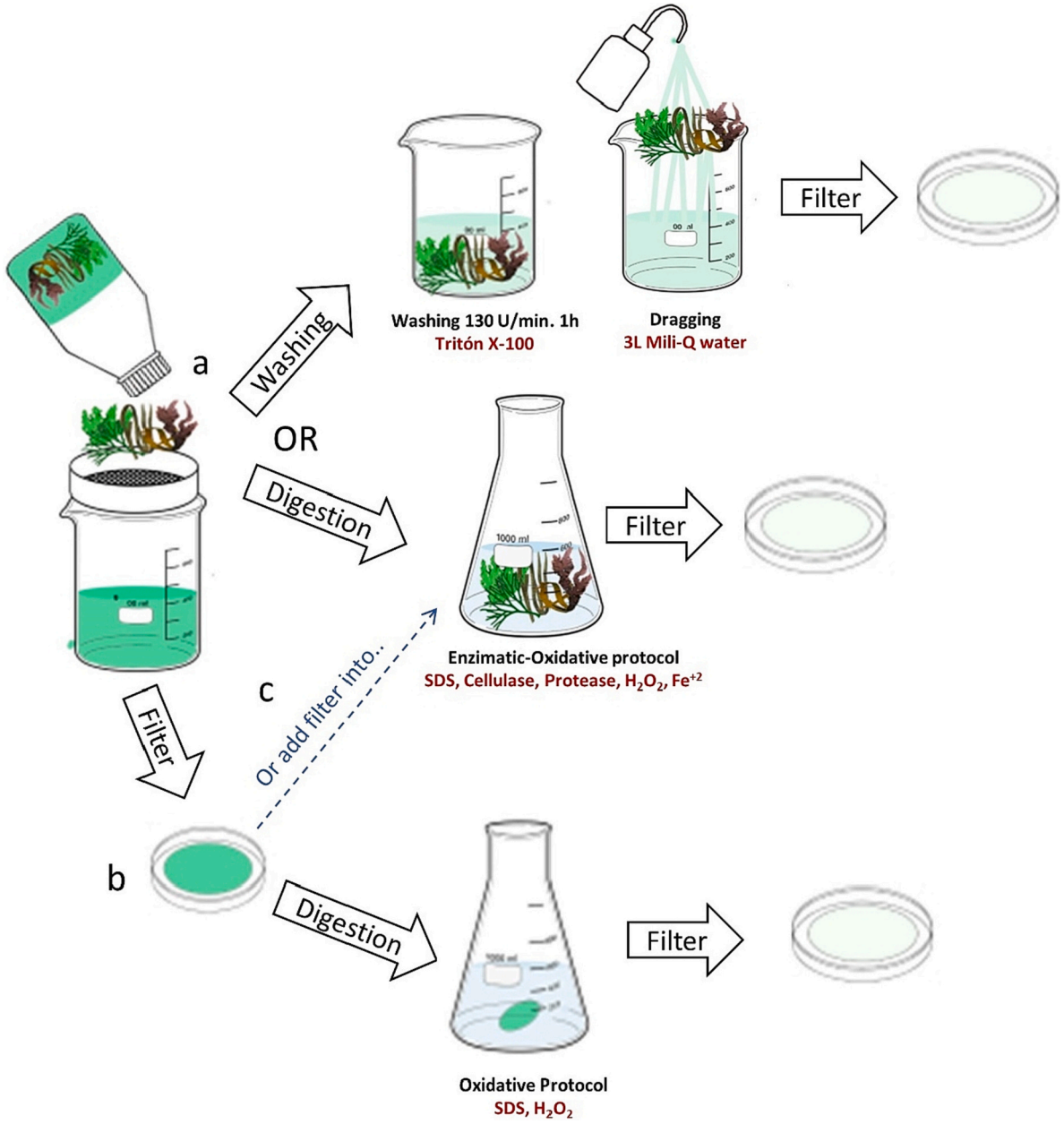

Fig. 3. Scheme of the sample treatment approaches studied in the paper, see text for details.

filter (20 μm pore, Fig. 3b). It was noticed that a soft digestion would be necessary because the filter was opaque, so we used the mild surfactant oxidative digestion proposed by López-Rosales et al. (2021) using 2 % SDS and 30 % H_2O_2 in 5 mL aliquots until reaching 15 % H_2O_2 in the final solution.

The algal phase was processed in two ways to compare two common procedures considered in literature (as resumed in the introduction): plain washing (Fig. 3a, "washing") and matrix digestion (Fig. 3a, "digestion"). They are detailed next.

3.3.1. *Washing macroalgae*

To study the washing procedure used quite frequently, the liquid phase was handled separately (Fig. 3b) to evaluate how many MPs were released into the water matrix (and how many became retained by the algal matrix). In case there is no interest on this separate evaluation, this step is not required anymore and the filter cake of the water phase can be added to the algal one during digestion (Fig. 3c).

As commented in the introductory sections, some researchers rely on rising the algae with water to remove MPs. This simple approach is far from being accepted and most people prefer to digest the organic matter of the algae. However it is worth considering this option because, if successful, it would be of low cost and only moderately labor-demanding. Sundbæk et al. (2018) demonstrated a 94.5 % reduction in the MPs adhered to the leafs after washing in a rotating box for 1 h. Similarly, Seng et al. (2020) and Goss et al. (2018) reported good results after direct observation of MPs on the leaves. On the contrary, Feng et al. (2020a) found that washing *P. yezoensis and U. pinnatifida* was not enough to detach MPs from their surface. Peller et al. (2021) observed that MPs remained adsorbed onto the algal surface after successive washings with water. Jones et al. (2020) proposed washing algae "dynamically" with distilled water in a centrifuge tube with vigorous shaking.

To get insight on this approach five spiked samples were prepared as detailed in Section 2.3 and treated as described in Fig. 3a: 300 mL of Triton X-100 (0.1 %) were used to clean the algal fragments by rotation (130 U/min, 1 h) and a subsequent thorough dragging with ca. 3 L of a 2

Table 3
Average recoveries, as %, (± standard deviation, n = 5) of the spiked MPs and fibres; 20 particles of each polymer were, 'All MPs' represents 140 items in total.

		PS	PP	PE	PET	PA	PVC	Fibres	All MP
Washing	Algae	11 ± 2	12 ± 3	17 ± 3	13 ± 3	14 ± 2	9 ± 10	9 ± 5	12 ± 2
	Water	61 ± 7	64 ± 5	65 ± 5	62 ± 3	72 ± 6	59 ± 5	53 ± 10	62 ± 3
	Total matrix	72 ± 8	76 ± 8	86 ± 2	75 ± 4	87 ± 6	69 ± 11	64 ± 7	75 ± 4
Digestion	Algae	20 ± 6	23 ± 6	25 ± 5	23 ± 8	22 ± 8	33 ± 6	27 ± 8	25 ± 3
	Water	70 ± 4	68 ± 6	65 ± 4	68 ± 6	70 ± 5	56 ± 7	58 ± 16	65 ± 3
	Total matrix	90 ± 4	91 ± 2	90 ± 6	91 ± 2	92 ± 7	89 ± 4	85 ± 8	90 ± 2

% SDS solution. Each algal fragment was picked up individually with metallic tweezers and rinsed carefully over a 20 μm filter. The contents of the flask were filtered through another 20 μm stainless-steel filter. The two filters were placed in Petri dishes, dried, and inspected for suspicious particles, which were characterized as detailed in Section 2.2.

The recoveries in the seaweeds and aqueous filtrates, as well as the overall recoveries (algae + water) were calculated. This allows us to estimate the MPs retention capability of the seaweeds, which is around 25 % after washing. The results for the washing and digestion protocols are compared at Table 3. Partial (20 particles of each polymer) and overall recoveries (140 particles in total) were calculated in quintuplicate. For this purpose, the particles over the filter were counted and characterized scanning the whole filter (no subsampling strategy).

Table 3 shows that the general behavior of all studied polymers seemed the same because although most MPs were found in the aqueous filtrate in both treatments, a relevant number of MPs remained in the algae, even after careful washing; around 30 % of the particles when washing and ca. 10 % when digesting them. This demonstrates the strong binding that can occur between the MPs and the surface of the algal leaves. The overall recoveries are in general good as they range from 64 % (PVC and fibres) to 86 % (PE). However, they are clearly higher and more homogeneous for the oxidative enzymatic digestion (detailed in the next section).

3.3.2. *Digestion of the macroalgae*

Preliminary studies in our laboratory demonstrated that seaweeds had very different behaviors, as expected because of their different structural composition. For example, *Porphyra* and *Undaria* algae are more proteinaceous, and *Laminaria* and *Fucus* have more fibre (Palasí, 2015), while wakame contains carrageenans and alginates. Therefore, a protocol developed for one type of seaweed may be invalid for another. Following, the focus here is on developing a unique protocol valid to release MPs from common seaweeds (or their mixtures). A practical constrain was further stated: to require only one final filtration step, in order to minimise losses when several filtration steps are considered (Nakajima et al., 2019). The destruction of the organic matter was evaluated visually over the filters.

Acid-oxidative treatments (proposed by Huang et al., 2020) were discarded here because they can destroy/damage polymers (Avio et al., 2015; Catarino et al., 2017; Claessens et al., 2013; Dehaut et al., 2016; Naidoo et al., 2017; Karami et al., 2017; Pfeiffer and Fischer, 2020).

3.3.2.1. Oxidative treatments. Oxidative treatments are quite popular to digest organic matter. Peller et al. (2021) used an oxidative medium (deionised water:H_2O_2; 3:2), 70 °C, with a UV lamp for 60–70 min to form hydroxyl radicals and accelerate oxidative degradation, and final shaking at room temperature. Feng et al. (2020a) used the Fenton's reagent (20 g FeSO4 7H_2O_2/L and 30 % H_2O_2; 1:1 and 1:2 volume ratios, 40 °C, 60 rpm for 48 h) to digest cultured macroalgae (*P. yezoensis, U. prolifera and S. horneri*) and *U. prolifera* (Feng et al., 2020a). Gao et al. (2020) destroyed successfully *U. prolifera* using 30 % H_2O_2. The problem here is that concentrated H_2O_2 (ca. 30 %) may damage some synthetic polymers (Crawford and Quinn, 2017; Lusher et al., 2017), up to a 16 % volume reduction of <1 mm PP, PE, PA, PC and PP particles (Nuelle et al., 2014). Strong PA6.6 and PS degradation (Hurley et al., 2018), as well as PET and PA fibres (Treilles et al., 2020) degradation; size reduction in PLA and, even, tyre rubber surface changes (Pfohl et al., 2021) and on PVC Raman spectra (Lenz et al., 2021) have been reported. Tsangaris et al. (2021) recommended 15 % H_2O_2 as compromise between polymer preservation and organic matter digestion.

An oxidative strategy was tested here following Feng et al. (2020a,b) and Peller et al. (2021) to treat wakame and sea spaghetti. Results were unsatisfactory because in both cases a thick layer of a gel-type semisolid matrix was obtained. Its IR spectrum coincided with different types of polysaccharides, and it was concluded that they may be phycocolloids (alginates, carrageenans, etc.).

The Fenton's reagent, used frequently to get a stronger oxidation medium, causes violent reactions and excessive foam and temperatures notably >40 °C (limit recommended by Lusher et al. (2020)). To ameliorate this problem here the oxidative digestion was done in a tiered way. In brief, 500 mL of 15 % H_2O_2 were added and incubated (130 U/min, 40 °C, 48 h). Then, the Fe^{+2} salt was added at a 0.20 g/6 h pace (room temperature) until completing 2.5 g. This procedure fits the suggestions given by Tagg et al. (2016), Al-Azzawi et al. (2020), Hurley et al. (2018) and Treilles et al. (2020) to preserve the integrity of polymeric fibres. To dissolve Fe^{+2} precipitates the pH was lowered to pH < 3, just before filtering. However, the results obtained for this approach were unsatisfactory as the filters clogged very rapidly and too many were needed per sample. Hence, this option was discarded.

3.3.2.2. Alkaline-oxidative treatment. The approach tried here is based on a previous one validated successfully for plankton and fish (López-Rosales et al., 2021). The protocol was modified slightly and the final setup was: 300 mL of 10 % KOH were added and incubated (40 °C, 130 U/min, 24 h), then 30 % H_2O_2 in 10 mL increments was added until obtaining a 15 % peroxide concentration in the final total volume. As for the previous approaches, the major problem was that an abundant gel-like material appeared in the filtrates requiring as many as 10 filters for some samples. Likely this material is formed –mainly- by algal wall debris and phycocolloids. This agrees with Pfeiffer and Fischer (2020) who stated that alkaline treatments are not suitable for samples with high proportions of cellulose, hemicellulose and lignin. Gao et al. (2020) couldn't digest *U. prolifera* because KOH only hydrolyse proteins. Also, it is worth noting that carrageenans present in algae precipitate in alkaline media (Diharmi et al., 2020).

3.3.2.3. Enzymatic treatment. Enzymatic methods appear as a "mild" and optimal way to keep MPs integrity, although they are time consuming and costly (Löder et al., 2017; Lusher et al., 2020). Therefore, they should be simplified as much as possible and, likely, combined with other reagents that can still preserve the integrity of the MPs.

To the best of our knowledge, only Li et al. (2020) applied enzymatic methods; in particular they digested dried Nori seaweeds by enzymolysis with cellulase to decompose the algal cytoderm, and alkalase to digest the proteins, followed by oxidation with 30 % H_2O_2. The enzymatic-oxidative treatment applied here is similar to López-Rosales et al. (2021): 2 % SDS, protease (500 μ/mL) and H_2O_2 up to 10 % of total volume, and based on the BEEP strategy from Löder et al. (2017). Since some problems persisted it was decided to use enzymes to break the bonds of the algal cell walls, as Li et al. (2020).

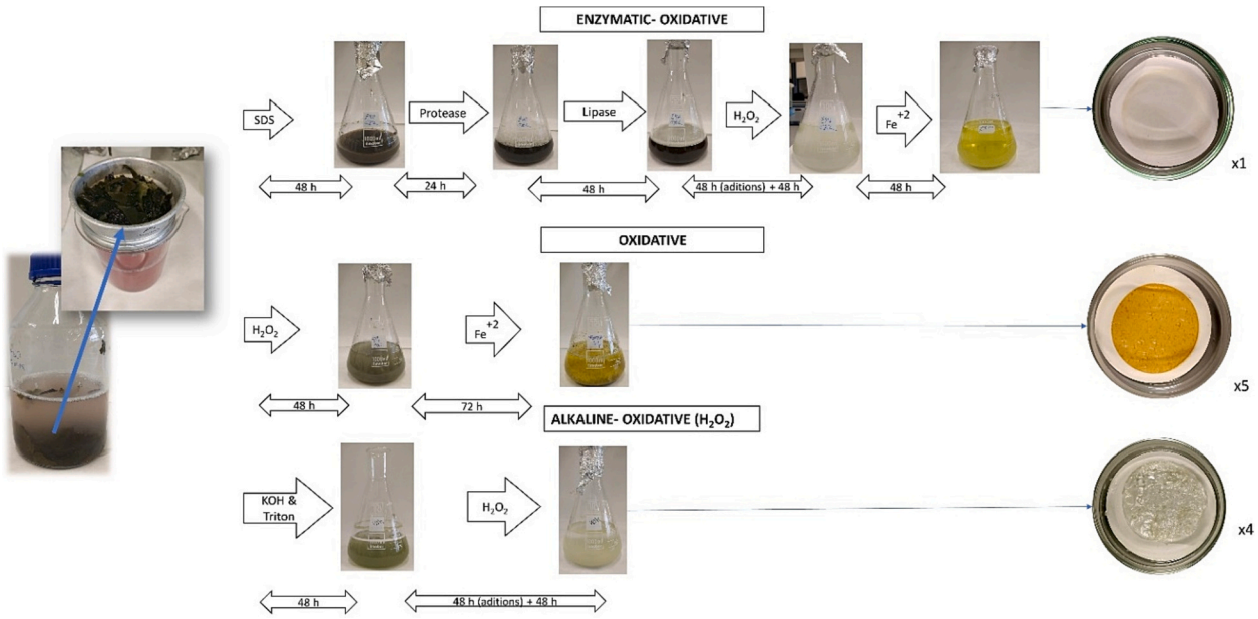

Fig. 4. Scheme of digestion protocols studied in this work (see text for details).

The protocol consists of adding 200 mL of a pH = 5 buffered solution (acetic acid/sodium acetate) and 3 g of cellulase to the sample and incubation (40 °C, 130 U/min, 48 h); then addition of 100 mL of 2 % SDS and incubation for 24 h. Subsequently, 40 mL of 1 M TRIS (which involved a previous adjustment to pH = 9) and 300 mg of protease were added and incubated for another 48 h. The oxidising phase was accomplished with 30 % H_2O_2, added in 10 mL increments until a total volume of 15 % is obtained (that required approx. 340 mL). The latter can take about 48 h as this step must be done carefully to avoid losses by foaming. Finally, the sample was incubated for 48 h. As the organic matter had not been oxidised totally jet (as per visual observation) the digestion and bleaching were completed with the Fenton's reagent; adding 0.20 g of the Fe^{+2} salt/4 h, at room temperature –four times- until the reaction stops. The suspension rested for another 24 h before filtration (just before filtering, the pH was adjusted to 3). The results were satisfactory because one filter was required and it had a nice visual appearance (no organic matrix remains), Fig. 4.

Recoveries were good, Table 3, around 90 % for all polymers, slightly lower for fibres, 85 %. Filter subsampling to speed up the measurements was also satisfactory, as recoveries were >83 % (Table 2). Visual changes in shape or color of the particles/fibres were not seen, and their spectra correlated highly with those of the same polymers in our spectral database, match indexes > 0.9. This is consistent with Philipp et al. (2022), Schrank et al. (2022), Pfohl et al. (2021) and Mbachu et al. (2021) who concluded that enzymatic digestions and the Fenton's reagent (either alone or combined) do not affect these common plastics in terms of spectral identification and changes of shape.

4. Conclusions

Three types of digestion methods were evaluated on a mixture of 5 commercial edible seaweeds where from the enzymatic-oxidative digestion one was selected. It was established as the most reliable one with good polymer recoveries (ca. 90 %) and visual absence of microplastics degradation. Further, this approach requires only one final filtration step to minimise losses. It was verified that a surfactant-based washing treatment was not satisfactory because around 20 % of the particles might still remain on the algal leaves.

The protocol proposed here can be applied whenever MPs can be searched for in both the algae and in the seawater where the seaweeds are, by separate. This allows the assessment of the microplastics retention capacity of the algae.

It was concluded that metallic filters yield better chemical identification of small particles and fibres than polymeric filters because they avoided background spectral interferences. A sub-sampling pattern that measures only 33,6 % of the 47 mm-diameter filter surface was proposed to accelerate the measuring process. This was validated for MPs ≤ 70 μm, and fibres. When this is combined with a manual approach to pick up MPs ≥ 70 μm it is possible to measure a filter (one sample) every 7–8 h (a working day).

Some future studies we can foresee to refine this study and go forward include evaluating whether the adsorption performance of the microplastics on the dried seaweeds after remixing with seawater is the same as that of fresh seaweeds. As this work was focused on commercial edible seaweeds it would be interesting to assess the behavior of wild macroalgae without any previous treatment. As a general issue for microplastics studies, it is important to search for new analytical approaches to reduce further the measuring time. Further some other common polymers would be studied, like, e.g., PU, PMMA or PA fibres, and biodegradable plastics (PLA, etc.). It would also be interesting to advance to lower particle size, like the 10–50 μm range.

CRediT authorship contribution statement

Conceptualization, methodology, validation and writing (review): all authors.

Software: ALR, JMA.

Formal analyses: ALR, JMA.

Investigation: ALR.

Resources, SML, PLM.

Writing draft: ALR, JMA, SML.

Declaration of competing interest

The authors declare that they have no known competing financial interests or personal relationships that could have appeared to influence the work reported in this paper.

Data availability

All relevant data have been presented into the text

Acknowledgements

This work is a part of the projects MicroplastiX (Grant PCI2020-112145, JPI Oceans Project supported by MCIN/AEI/10.13039/501100011033 and by the European Union "Next Generation EU/PRTR") and LAnd-Based solutions for PLAStics in the Sea, LABPLAS, (Grant H2020-101003954 supported by the EU H2020 program). The Program "Consolidación e Estructuración de Unidades de Investigación Competitivas" of the Galician Government (Xunta de Galicia) is also acknowledged (Grant ED431C 2021/56). Funding for open access charge: Universidade da Coruña/CISUG.

References

Al-Azzawi, M.S.M., Kefer, S., Weißer, J., Reichel, J., Schwaller, C., Glas, K., Knoop, O., Drewes, J.E., 2020. Validation of sample preparation methods for microplastic analysis in wastewater matrices—reproducibility and standardization. Water 12, 2445. https://doi.org/10.3390/w12092445.

Andrade, J.M., Ferreiro, B., López-Mahía, P., Muniategui-Lorenzo, S., 2020. Standardization of the minimum information for publication of infrared-related data when microplastics are characterized. Mar. Pollut. Bull. 154, 111035 https://doi.org/10.1016/j.marpolbul.2020.111035.

Avio, C.G., Gorbi, S., Regoli, F., 2015. Experimental development of a new protocol for extraction and characterization of microplastics in fish tissues: First observations in commercial species from Adriatic Sea. Mar. Environ. Res. 111, 18–26. https://doi.org/10.1016/j.marenvres.2015.06.014.

Bertelli, C.M., Unsworth, R.K.F., 2014. Protecting the hand that feeds us: seagrass (Zostera marina) serves as commercial juvenile fish habitat. Mar. Pollut. Bull. 83, 425–429. https://doi.org/10.1016/j.marpolbul.2013.08.011.

Bhattacharya, P., Lin, S., Turner, J.P., Ke, P.C., 2010. Physical adsorption of charged plastic nanoparticles affects algal photosynthesis. J. Phys. Chem. C 114, 16556–16561. https://doi.org/10.1021/jp1054759.

Blanco Murillo, F., 2018. Evolución y estado actual de las praderas de Posidonia oceanica (L.) Delile en la provincia de Alicante (Mediterráneo occidental).

Boney, A.D., 1978. Marine algae as collectors of iron ore dust. Mar. Pollut. Bull. 9, 175–180. https://doi.org/10.1016/0025-326X(78)90174-1.

Brandt, J., Bittrich, L., Fischer, F., Kanaki, E., Tagg, A., Lenz, R., Labrenz, M., Brandes, E., Fischer, D., Eichhorn, K.-J., 2020. High-throughput analyses of microplastic samples using fourier transform infrared and raman spectrometry. Appl. Spectrosc. 74, 1185–1197. https://doi.org/10.1177/0003702820932926.

Brandt, J., Fischer, F., Kanaki, E., Enders, K., Labrenz, M., Fischer, D., 2021. Assessment of subsampling strategies in microspectroscopy of environmental microplastic samples. Front. Environ. Sci. 8 https://doi.org/10.3389/fenvs.2020.579676.

Carretero, O., Gago, J., Filgueiras, A.V., Viñas, L., 2022. The seasonal cycle of micro and meso-plastics in surface waters in a coastal environment (Ría de Vigo, NW Spain). Sci. Total Environ. 803, 150021 https://doi.org/10.1016/j.scitotenv.2021.150021.

Catarino, A.I., Thompson, R., Sanderson, W., Henry, T.B., 2017. Development and optimization of a standard method for extraction of microplastics in mussels by enzyme digestion of soft tissues. Environ. Toxicol. Chem. 36, 947–951. https://doi.org/10.1002/etc.3608.

Claessens, M., Van Cauwenberghe, L., Vandegehuchte, M.B., Janssen, C.R., 2013. New techniques for the detection of microplastics in sediments and field collected organisms. Mar. Pollut. Bull. 70, 227–233. https://doi.org/10.1016/j.marpolbul.2013.03.009.

Cozzolino, L., Nicastro, K.R., Zardi, G.I., de los Santos, C.B., 2020. Species-specific plastic accumulation in the sediment and canopy of coastal vegetated habitats. Sci. Total Environ. 723, 138018 https://doi.org/10.1016/j.scitotenv.2020.138018.

Crawford, C.B., Quinn, B., 2017. In: Crawford, C.B., Quinn, B. (Eds.), Microplastic Pollutants, 9. Elsevier, pp. 203–218. https://doi.org/10.1016/B978-0-12-809406-8.00009-8.

Dehaut, A., Cassone, A.-L., Frère, L., Hermabessiere, L., Himber, C., Rinnert, E., Rivière, G., Lambert, C., Soudant, P., Huvet, A., Duflos, G., Paul-Pont, I., 2016. Microplastics in seafood: Benchmark protocol for their extraction and characterization. Environ. Pollut. 215, 223–233. https://doi.org/10.1016/j.envpol.2016.05.018.

Diharmi, A., Rusnawati, Irasari, N., 2020. Characteristic of carrageenan Eucheuma cottonii collected from the coast of Tanjung Medang Village and Jaga Island, Riau. IOP Conf. Ser.: Earth Environ. Sci. 404, 012049 https://doi.org/10.1088/1755-1315/404/1/012049.

Enders, K., Lenz, R., Ivar do Sul, J.A., Tagg, A.S., Labrenz, M., 2020. When every particle matters: a QuEChERS approach to extract microplastics from environmental samples. MethodsX 7, 100784. https://doi.org/10.1016/j.mex.2020.100784.

Feng, Z., Zhang, T., Shi, H., Gao, K., Huang, W., Xu, J., Wang, J., Wang, R., Li, J., Gao, G., 2020a. Microplastics in bloom-forming macroalgae: distribution, characteristics and impacts. J. Hazard. Mater. 397, 122752 https://doi.org/10.1016/j.jhazmat.2020.122752.

Feng, Z., Zhang, T., Wang, J., Huang, W., Wang, R., Xu, J., Fu, G., Gao, G., 2020. Spatio-temporal features of microplastics pollution in macroalgae growing in an important mariculture area, China. Sci. Total Environ. 719, 137490 https://doi.org/10.1016/j.scitotenv.2020.137490.

Franco, A.A., Arellano, J.M., Albendín, G., Rodríguez-Barroso, R., Zahedi, S., Quiroga, J. M., Coello, M.D., 2020. Mapping microplastics in Cadiz (Spain): occurrence of microplastics in municipal and industrial wastewaters. J. Water Process Eng. 38, 101596 https://doi.org/10.1016/j.jwpe.2020.101596.

Gao, F., Li, J., Hu, J., Li, X., Sun, C., 2020. Occurrence of microplastics carried on Ulva prolifera from the Yellow Sea, China. Case Stud. Chem. Environ. Eng. 2, 100054 https://doi.org/10.1016/j.cscee.2020.100054.

Gao, G., Gao, Q., Bao, M., Xu, J., Li, X., 2019. Nitrogen availability modulates the effects of ocean acidification on biomass yield and food quality of a marine crop pyropia yezoensis. Food Chem. 271, 623–629. https://doi.org/10.1016/j.foodchem.2018.07.090.

Gao, G., Gao, L., Jiang, M., Jian, A., He, L., 2021a. The potential of seaweed cultivation to achieve carbon neutrality and mitigate deoxygenation and eutrophication. Environ. Res. Lett. 17, 014018 https://doi.org/10.1088/1748-9326/ac3fd9.

Gao, G., Zhao, X., Jin, P., Gao, K., Beardall, J., 2021b. Current understanding and challenges for aquatic primary producers in a world with rising micro- and nano-plastic levels. J. Hazard. Mater. 406, 124685 https://doi.org/10.1016/j.jhazmat.2020.124685.

Goss, H., Jaskiel, J., Rotjan, R., 2018. Thalassia testudinum as a potential vector for incorporating microplastics into benthic marine food webs. Mar. Pollut. Bull. 135, 1085–1089. https://doi.org/10.1016/j.marpolbul.2018.08.024.

Gutow, L., Eckerlebe, A., Giménez, L., Saborowski, R., 2016a. Experimental evaluation of seaweeds as a vector for microplastics into marine food webs. Environ. Sci. Technol. 50, 915–923. https://doi.org/10.1021/acs.est.5b02431.

Hämer, J., Gutow, L., Köhler, A., Saborowski, R., 2014. Fate of microplastics in the marine isopod Idotea emarginata. Environ. Sci. Technol. 48, 13451–13458. https://doi.org/10.1021/es501385y.

Hermsen, E., Mintening, S.M., Besseling, E., Koelmans, A.A., 2018. Quality criteria for the analysis of microplastic in biota samples: A critical review. Environ. Sci. Technol 52, 10230–10240. https://doi.org/10.1021/acs.est.8b01611.

Huang, Y., Xiao, X., Xu, C., Perianen, Y.D., Hu, J., Holmer, M., 2020. Seagrass beds acting as a trap of microplastics - emerging hotspot in the coastal region? Environ. Pollut. 257, 113450 https://doi.org/10.1016/j.envpol.2019.113450.

Huppertsberg, S., Knepper, T.P., 2020. Validation of an FT-IR microscopy method for the determination of microplastic particles in surface waters. MethodsX 7, 100874. https://doi.org/10.1016/j.mex.2020.100874.

Hurley, R.R., Lusher, A.L., Olsen, M., Nizzetto, L., 2018. Validation of a method for extracting microplastics from complex, organic-rich, environmental matrices. Environ. Sci. Technol. 52, 7409–7417. https://doi.org/10.1021/acs.est.8b01517.

Jones, K.L., Hartl, M.G.J., Bell, M.C., Capper, A., 2020. Microplastic accumulation in a Zostera marina L. bed at deerness sound, Orkney, Scotland. Mar. Pollut. Bull. 152, 110883 https://doi.org/10.1016/j.marpolbul.2020.110883.

Karami, A., Golieskardi, A., Choo, C.K., Romano, N., Ho, Y.B., Salamatinia, B., 2017. A high-performance protocol for extraction of microplastics in fish. Sci. Total Environ. 578, 485–494. https://doi.org/10.1016/j.scitotenv.2016.10.213.

Lenz, R., Enders, K., Fischer, F., Brandt, J., Fischer, D., Labrenz, M., 2021. Measuring impacts of microplastic treatments via image recognition on immobilised particles below 100 μm. Microplas. Nanoplas. 1, 12. https://doi.org/10.1186/s43591-021-00012-0.

Li, Q., Feng, Z., Zhang, T., Ma, C., Shi, H., 2020a. Microplastics in the commercial seaweed nori. J. Hazard. Mater. 388, 122060 https://doi.org/10.1016/j.jhazmat.2020.122060.

Li, Q., Su, L., Ma, C., Feng, Z., Shi, H., 2022. Plastic debris in coastal macroalgae. Environ. Res. 205, 112464 https://doi.org/10.1016/j.envres.2021.112464.

Liu, K., Wang, X., Wei, N., Song, Z., Li, D., 2019. Accurate quantification and transport estimation of suspended atmospheric microplastics in megacities: implications for human health. Environ. Int. 132, 105127 https://doi.org/10.1016/j.envint.2019.105127.

Löder, M.G.J., Imhof, H.K., Ladehoff, M., Löschel, L.A., Lorenz, C., Mintenig, S., Piehl, S., Primpke, S., Schrank, I., Laforsch, C., Gerdts, G., 2017. Enzymatic purification of microplastics in environmental samples. Environ. Sci. Technol. 51, 14283–14292. https://doi.org/10.1021/acs.est.7b03055.

López-Rosales, A., Andrade, J.M., Grueiro-Noche, G., Fernández-González, V., López-Mahía, P., Muniategui-Lorenzo, S., 2021. Development of a fast and efficient method to analyze microplastics in planktonic samples. Mar. Pollut. Bull. 168, 112379 https://doi.org/10.1016/j.marpolbul.2021.112379.

Lusher, A.L., Welden, N.A., Sobral, P., Cole, M., 2017. Sampling, isolating and identifying microplastics ingested by fish and invertebrates. Anal. Methods 9, 1346–1360. https://doi.org/10.1039/C6AY02415G.

Lusher, A.L., Munno, K., Hermabessiere, L., Carr, S., 2020a. Isolation and extraction of microplastics from environmental samples: an evaluation of practical approaches and recommendations for further harmonization. Appl. Spectrosc. 74, 1049–1065. https://doi.org/10.1177/0003702820938993.

Mbachu, O., Jenkins, G., Pratt, C., Kaparaju, P., 2021. Enzymatic purification of microplastics in soil. MethodsX 8, 101254. https://doi.org/10.1016/j.mex.2021.101254.

Mendoza, A., Osa, J.L., Basurko, O.C., Rubio, A., Santos, M., Gago, J., Galgani, F., Peña-Rodriguez, C., 2020. Microplastics in the Bay of Biscay: an overview. Mar. Pollut. Bull. 153, 110996 https://doi.org/10.1016/j.marpolbul.2020.110996.

Naidoo, T., Goordiyal, K., Glassom, D., 2017. Are nitric acid (HNO3) digestions efficient in isolating microplastics from juvenile fish? Water. Air. Soil Pollut. 228, 470. https://doi.org/10.1007/s11270-017-3654-4.

Nakajima, R., Lindsay, D.J., Tsuchiya, M., Matsui, R., Kitahashi, T., Fujikura, K., Fukushima, T., 2019. A small, stainless-steel sieve optimized for laboratory beaker-based extraction of microplastics from environmental samples. MethodsX 6, 1677–1682. https://doi.org/10.1016/j.mex.2019.07.012.

Nolte, T.M., Hartmann, N.B., Kleijn, J.M., Garnæs, J., van de Meent, D., Jan Hendriks, A., Baun, A., 2017. The toxicity of plastic nanoparticles to green algae as influenced by

surface modification, medium hardness and cellular adsorption. Aquat. Toxicol. 183, 11–20. https://doi.org/10.1016/j.aquatox.2016.12.005.
Nuelle, M.-T., Dekiff, J.H., Remy, D., Fries, E., 2014. A new analytical approach for monitoring microplastics in marine sediments. Environ. Pollut. 184, 161–169. https://doi.org/10.1016/j.envpol.2013.07.027.
Peller, J., Nevers, M.B., Byappanahalli, M., Nelson, C., Ganesh Babu, B., Evans, M.A., Kostelnik, E., Keller, M., Johnston, J., Shidler, S., 2021. Sequestration of microfibers and other microplastics by green algae, cladophora, in the US Great Lakes. Environ. Pollut. 276, 116695 https://doi.org/10.1016/j.envpol.2021.116695.
Palasí, J.T., Fernández-Segovia, I., Fuentes, A., 2015. Caracterización físico-química y nutricional de algas en polvo empleadas como ingrediente alimentario. http://hdl.handle.net/10251/55641. (Accessed 24 August 2022).
Peller, J.R., Eberhardt, L., Clark, R., Nelson, C., Kostelnik, E., Iceman, C., 2019. Tracking the distribution of microfiber pollution in a southern Lake Michigan watershed through the analysis of water, sediment and air. Environ Sci Process Impacts 21, 1549–1559. https://doi.org/10.1039/C9EM00193J.
Peñalver, R., Lorenzo, J.M., Ros, G., Amarowicz, R., Pateiro, M., Nieto, G., 2020. Seaweeds as a functional ingredient for a healthy diet. Mar. Drugs 18. https://doi.org/10.3390/md18060301.
Peteiro, C., García Tasende, M., 2015. In: Uso y cultivo de laminarias, las grandes algas marinas. Investigacion y ciencia, 466, pp. 8–9.
Pfeiffer, F., Fischer, E.K., 2020. Various digestion protocols within microplastic sample processing—evaluating the resistance of different synthetic polymers and the efficiency of biogenic organic matter destruction. Front. Environ. Sci. 8 https://doi.org/10.3389/fenvs.2020.572424.
Pfohl, P., Roth, C., Meyer, L., Heinemeyer, U., Gruendling, T., Lang, C., Nestle, N., Hofmann, T., Wohlleben, W., Jessl, S., 2021. Microplastic extraction protocols can impact the polymer structure. Microplast. Nanoplast. 1, 8. https://doi.org/10.1186/s43591-021-00009-9.
Philipp, M., Bucheli, T.D., Kaegi, R., 2022. The use of surrogate standards as a QA/QC tool for routine analysis of microplastics in sewage sludge. Sci. Total Environ. 835, 155485 https://doi.org/10.1016/j.scitotenv.2022.155485.
Picó, Y., Barceló, D., 2019. Analysis and prevention of microplastics pollution in water: current perspectives and future directions. ACS Omega 4, 6709–6719. https://doi.org/10.1021/acsomega.9b00222.
Remy, F., Collard, F., Gilbert, B., Compère, P., Eppe, G., Lepoint, G., 2015. When microplastic is not plastic: the ingestion of artificial cellulose fibers by macrofauna living in seagrass macrophytodetritus. Environ. Sci. Technol. 49, 11158–11166. https://doi.org/10.1021/acs.est.5b02005.
Roberts, D.A., Poore, A.G.B., Johnston, E.L., 2006. Ecological consequences of copper contamination in macroalgae: effects on epifauna and associated herbivores. Environ. Toxicol. Chem. 25, 2470–2479. https://doi.org/10.1897/05-661r.1.
Rodrigues, S.M., Elliott, M., Almeida, C.M.R., Ramos, S., 2021. Microplastics and plankton: knowledge from laboratory and field studies to distinguish contamination from pollution. J. Hazard. Mater. 417, 126057 https://doi.org/10.1016/j.jhazmat.2021.126057.
Sana, S.S., Dogiparthi, L.K., Gangadhar, L., Chakravorty, A., Abhishek, N., 2020. Effects of microplastics and nanoplastics on marine environment and human health. Environ. Sci. Pollut. Res. 27, 44743–44756. https://doi.org/10.1007/s11356-020-10573-x.
Schrank, I., Möller, J.N., Imhof, H.K., Hauenstein, O., Zielke, F., Agarwal, S., Löder, M.G.J., Greiner, A., Laforsch, C., 2022. Microplastic sample purification methods - assessing detrimental effects of purification procedures on specific plastic types. Sci. Total Environ. 154824 https://doi.org/10.1016/j.scitotenv.2022.154824.
Seng, N., Lai, S., Fong, J., Saleh, M.F., Cheng, C., Cheok, Z.Y., Todd, P.A., 2020. Early evidence of microplastics on seagrass and macroalgae. Mar. Freshw. Res. 71, 922–928. https://doi.org/10.1071/MF19177.
Sundbæk, K.B., Koch, I.D.W., Villaro, C.G., Rasmussen, N.S., Holdt, S.L., Hartmann, N.B., 2018. Sorption of fluorescent polystyrene microplastic particles to edible seaweed Fucus vesiculosus. J. Appl. Phycol. 30, 2923–2927. https://doi.org/10.1007/s10811-018-1472-8.
Tagg, A.S., Harrison, J.P., Ju-Nam, Y., Sapp, M., Bradley, E.L., Sinclair, C.J., Ojeda, J.J., 2016. Fenton's reagent for the rapid and efficient isolation of microplastics from wastewater. Chem. Commun. 53, 372–375. https://doi.org/10.1039/C6CC08798A.
Treilles, R., Cayla, A., Gaspéri, J., Strich, B., Ausset, P., Tassin, B., 2020. Impacts of organic matter digestion protocols on synthetic, artificial and natural raw fibers. Sci. Total Environ. 748, 141230 https://doi.org/10.1016/j.scitotenv.2020.141230.
Tsangaris, C., Panti, C., Compa, M., Pedà, C., Digka, N., Baini, M., D'Alessandro, M., Alomar, C., Patsiou, D., Giani, D., Romeo, T., Deudero, S., Fossi, M.C., 2021. Interlaboratory comparison of microplastic extraction methods from marine biota tissues: A harmonization exercise of the Plastic Busters MPAs project. Mar. Pollut. Bull. 164, 111992. https://doi.org/10.1016/j.marpolbul.2021.111992.
Walkinshaw, C., Lindeque, P.K., Thompson, R., Tolhurst, T., Cole, M., 2020. Microplastics and seafood: lower trophic organisms at highest risk of contamination. Ecotoxicol. Environ. Saf. 190, 110066 https://doi.org/10.1016/j.ecoenv.2019.110066.
Weis, J.S., 2019. Improving microplastic research. AIMS Environ. Sci. 6, 326. https://doi.org/10.3934/environsci.2019.5.326.
Yu, Q., Hu, X., Yang, B., Zhang, G., Wang, J., Ling, W., 2020. Distribution, abundance and risks of microplastics in the environment. Chemosphere, 126059. https://doi.org/10.1016/j.chemosphere.2020.126059.